Performance Modelling of a Pressure Gain Combustion Aircraft Engine

Sreenath Purushothaman[1], Alessandro Sorce[2], Alberto Traverso[3]
DIME – University of Genova, Via Montallegro 1, Genova 16145, Italy

Thomas Gaillard[4] and Dmitry Davidenko [5]
DMPE, ONERA, Université Paris Saclay, F-91123 Palaiseau - France

As the gas turbine designs used today are reaching the limits of their performance, despite various optimization techniques adopted in recent years, the need arises for new types of propulsion devices. Pressure Gain Combustion (PGC) technology is an actively pursued area of innovation for gas turbine cycles that can be implemented in aerospace propulsion and land-based power generation. The advantages of pressure gain combustion, such as higher thermodynamic cycle efficiency and lower specific fuel consumption, make it an attractive alternative to conventional Brayton cycle, which uses constant pressure heat addition. Various pressure gain combustion technologies such as Pulse Detonation Engines (PDE) and Rotating Detonation Engine (RDE) are currently being investigated for propulsion applications, either as standalone propulsive devices or as constant pressure - PGC hybrid engines. Based on specific engine data, this paper aims at assessing the performance of pressure gain combustion in the framework of aircraft propulsion using the in-house simulation tool 'TRANSEO'.

I. Nomenclature

CJ	=	Pertaining to Chapman-Jouguet condition
C_p	=	Specific heat at constant pressure
M	=	Mach number
$\boldsymbol{q}_{\text{in}}$	=	Heat addition
$\tilde{\boldsymbol{q}}$	=	Non-dimensional heat addition
T	=	Static temperature
T_0	=	Stagnation temperature
s	=	Entropy
γ	=	Ratio of specific heats
ψ	=	Non-dimensional compressor temperature ratio

II. Introduction

Pressure gain combustion (PGC) devices operate on either constant volume cycle (Humphrey cycle), as in the case of wave rotors, or on detonation cycle, as in the case of pulse detonation engines (PDE) and rotating detonation engines (RDE). These cycles have better thermodynamic efficiency and lower specific fuel consumption as compared to conventional gas turbine engines operating on ideal Brayton cycle [1], under the same initial state and same specific heat addition (Fig. 1)[2]. Moreover, RDE stands out amongst the pressure gain combustion devices, due to their shorter length and flexibility in turbomachinery integration owing to their continuous detonation operation. Hence, it is

[1] PhD Student, DIME - University of Genova, Italy, Student Member.
[2] Associate Professor, DIME - University of Genova, Italy.
[3] Full professor, DIME - University of Genova, Italy.
[4] Senior research engineer, DMPE, ONERA, Université Paris Saclay, F-91123 Palaiseau - France
[5] Specialist research engineer, DMPE, ONERA, Université Paris Saclay, F-91123 Palaiseau - France

preferred over pulse detonation engines for civil aviation operations by many researchers. This study focuses on a generic detonation cycle pressure gain combustion technology that can be used for aircraft propulsion engines.

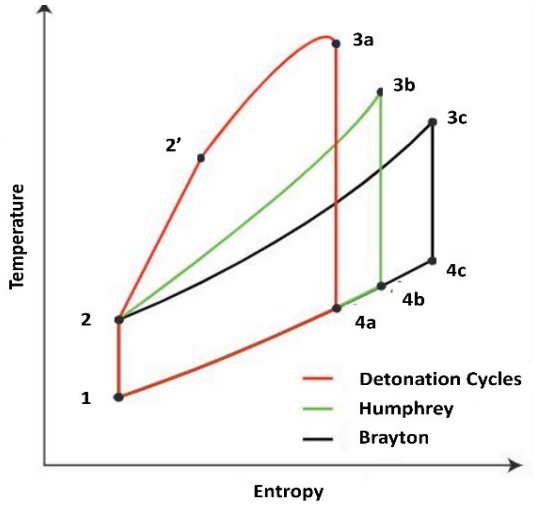

Fig. 1 Temperature–Entropy diagrams for the ideal Detonation, Brayton, and Humphrey cycles [2]

III. Literature review

A. Pressure Gain Combustion for propulsion

A number of studies have been reported in literature on the possible application of pressure gain combustion to replace the conventional gas turbine engines [3]. Studies by Stathopoulos [4,5] and Stechmann [6] are some of the recent attempts in this area. Experimental studies on RDE for space applications such as [7] and [8,9] have been reported to be successfully completed as well. Yet, the application of pressure gain combustion for aircraft propulsion is an area that is still under investigation. The difficulties facing the development of such engines include turbomachinery integration [10–12], fuel flexibility [13,14], cooling [15] and control system development.

B. Aircraft Engine modelling

There have been a number of efforts to model aircraft propulsion systems throughout the years. This includes, but not limited to, the works by Alexiou [16], Khalil et.al [17], Sankar et. al[18] , Carcasci et.al [19,20] Martins [21] and Ridaura [22]. These approaches usually use commercial software like GasTurb or Gas turbine Simulation Program (GSP) to predict the performance of the engine. Matlab/Simulink based tools are also being used in these works to simulate aircraft engines.

Most of the published works use lumped volume approach for transient simulations. This is where the TRANSEO simulation tool shines, when needed, as it is cable of capturing the effects of internal fluid dynamics as well. Unfortunately, the engine manufacturers are unwilling to provide the detailed geometric and performance data that is required for the dynamic simulation. The data used in this activity has been taken from the literature that is available in the public domain, with reasonable assumptions about the unknown variables.

C. TRANSEO Simulation tool

TRANSEO is a MATLAB-Simulink-based simulation tool capable of transient and dynamic simulation of systems, developed by the Thermochemical Power Group of University of Genova, Italy. It is designed for simulating systems operating with different cycles and different sizes. It has been successfully employed in the study of microturbine-based energy systems, as in [23] and [24] , and hybrid fuel cell systems, as in [25], and for supercritical CO2 cycles [26] as well. The TRANSEO tool has over 30 inbuilt modules, along with standardized interconnecting protocols for assembling the modules to obtain the desired system layout. The tool organization is shown in Fig. 2. All the modules are capable for both on-design and off-design static analysis and lumped-volume analysis. A few modules are also provided with 1-D dynamic simulation capability and real-time deployment as well.

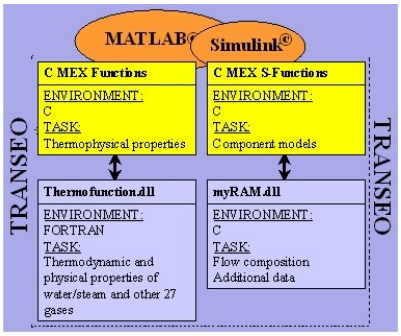

Fig. 2 TRANSEO organization [27]

IV. Modelling Methodology

The study reported in this paper begins by modelling a conventional gas turbine used for civil aviation applications using TRANSEO. The characteristic maps of fan, low-pressure compressor, high-pressure compressor, high-pressure turbine, and low-pressure turbine are used as primary inputs to the model. Additional inputs such as fuel injection parameters, component geometry and heat transfer details are also required along with details of compressor air bleed. The performance of the engine predicted by the model is then validated against the experimental data to a reasonable extent. This demonstrates the capability of the TRANSEO code to successfully model conventional aircraft gas turbine engines.

The next step in the study is the modelling of a modified version of the original aircraft engine with pressure gain combustion. For this purpose, a new combustor module is developed in the TRANSEO library that can represent pressure gain combustion, as a simple lumped volume model, without taking into account the complicated detonation chemistry and flow instabilities inside the combustion chamber. A simple PGC propulsion engine layout is also developed to study the engine performance.

A. CFM56-3 engine modelling using TRANSEO Simulation tool

The aircraft engine modelled using TRANSEO is a typical high-bypass turbofan engine used in civilian aircraft. In order to validate the model, the CFM56-3 engine manufactured by CFM International is used. The choice of this engine is due to the fact that a substantial amount of data on its performance is available in the public domain. The missing data such as component geometry, heat transfer from components, fuel composition etc. have been approximated to a reasonable value. The model is validated at the on-design & off-design points, where performance data was available, as reported by Ridaura [22].

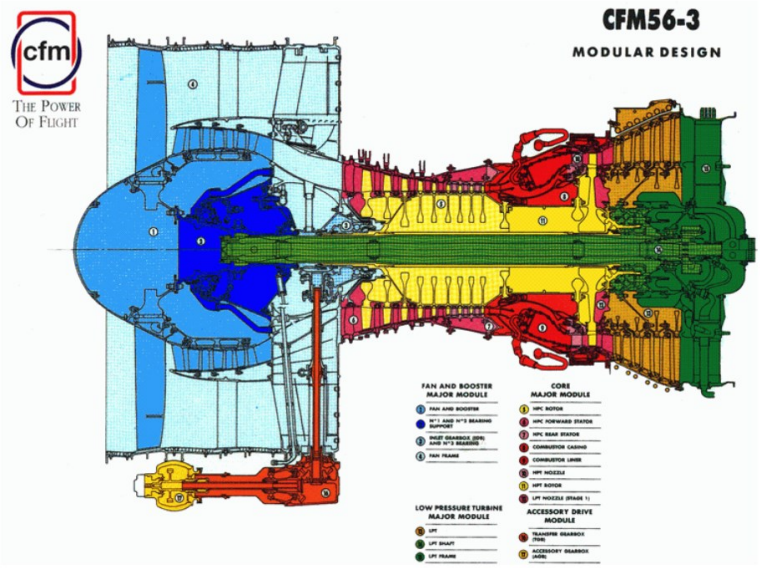

Fig. 3 CFM56-3 Schematic [21]

A typical CFM56-3 engine construction is shown in Fig. . The single stage high pressure turbine (HPT) drives the 9-stage high pressure compressor (HPC), which rotates at HP spool speed N2. The annular combustion chamber (CC) is fed by 20 fuel injectors, which is mixed with the air from the 9th stage of the HPC. The 4-stage low pressure turbine drives the fan and 3 stage low pressure compressor (LPC), rotating at LP spool speed N1. In addition, there are 12 variable bleed valves (VBV) located in the fan structure and between the LPC and HPC to account for the engine transient operation. There are also 4 variable stator vanes (VSV) and 5 outlet guide vanes (OGV) in the HPC. In addition to this, the secondary air-system of the engine is also designed to provide cooling to the HPT & LPT nozzle guide vane (NGV) and HPT rotors, and for the blade tip clearance control. For the simulation, a generic fuel of lower heating value (LHV) of 43.4 MJ/kg is selected for the conventional engine. In addition, a nozzle efficiency of 0.955 is calculated from the experimental data for both core and bypass nozzles.

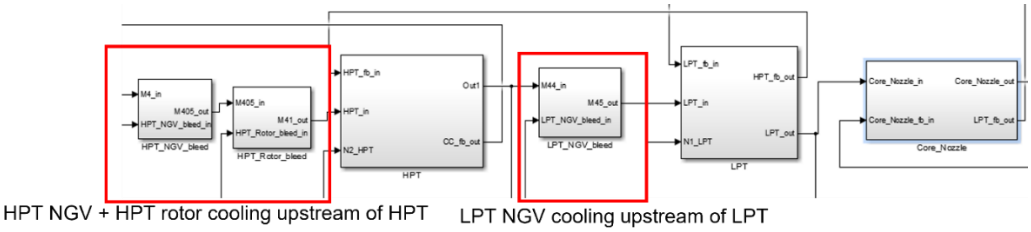

Fig. 4 Cooling methodology for Type 1 model

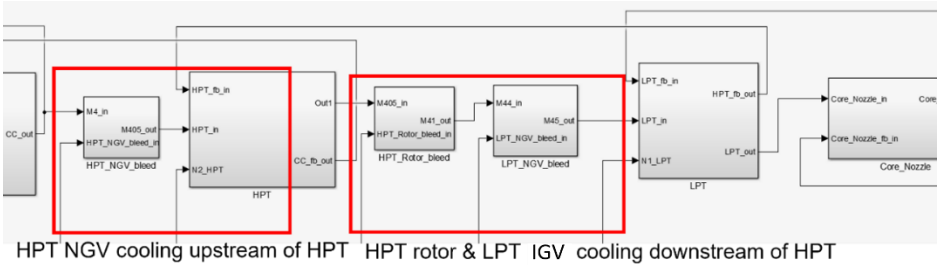

Fig. 5 Cooling methodology for Type 2 model

The details of the bleed schedule are not directly available from the engine manufacturer, but a good approximation at high engine spool speeds is available in literature [22]. Using this data and an approximated geometry of the engine components, two different bleed models, named Type 1 (Fig.) and Type 2 (Fig.), are developed and compared against the experimental data from Ridaura [22]. The model which closely resembles the experimental data (Type 2) is selected for further studies (Fig.).

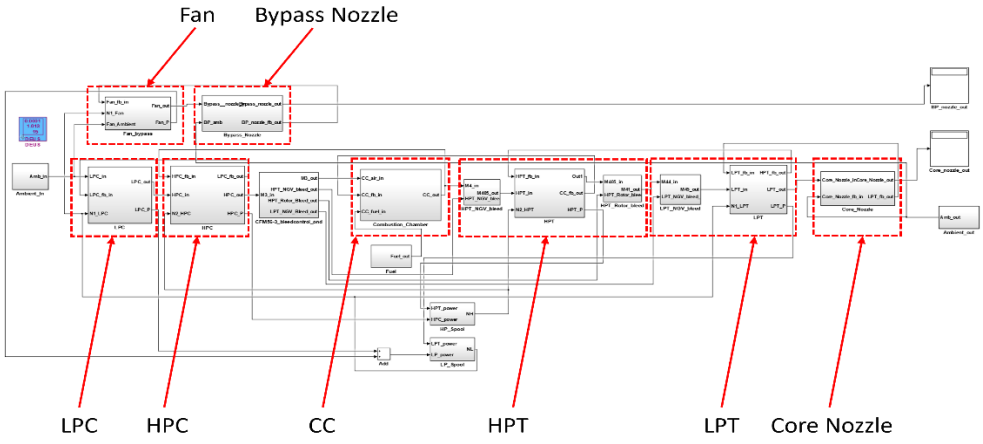

Fig. 6 CFM56-3 engine model in TRANSEO

The next step of the study involved validation of the TRANSEO model for off-design points. 15 points in the performance map, as reported by Ridaura [22], were selected for comparison with the TRANSEO simulation results. These results were found to be within an acceptable margin of error. Thus, TRANSEO modelling technique was deemed satisfactory to simulate aircraft engines, and thereby allowing the authors to proceed with confidence to model PGC propulsion engine.

B. Pressure gain combustion engine modelling

In order to model a PGC engine, a simple cycle layout is developed. The layout (Fig.) consists of a primary compressor (C1), a booster compressor (C2), a fan, high-pressure (T1) and low-pressure (T2) turbines, RDE combustor, and 6 mass flow splitters (indicated by red, green and blue circles) and a mixer. The mass flow splitters divide the compressor delivery air flow to different components to obtain the required temperature for turbine inlet. The mixer at combustor outlet is designed in such a way that a Mach number of 0.5 is obtained at the T1 inlet. The RDE combustor consists of a fuel-air injection pressure loss model and an equilibrium chemical kinetics map for detonation combustion at different fuel-air equivalence ratios and for an exit Mach number of 0.8.

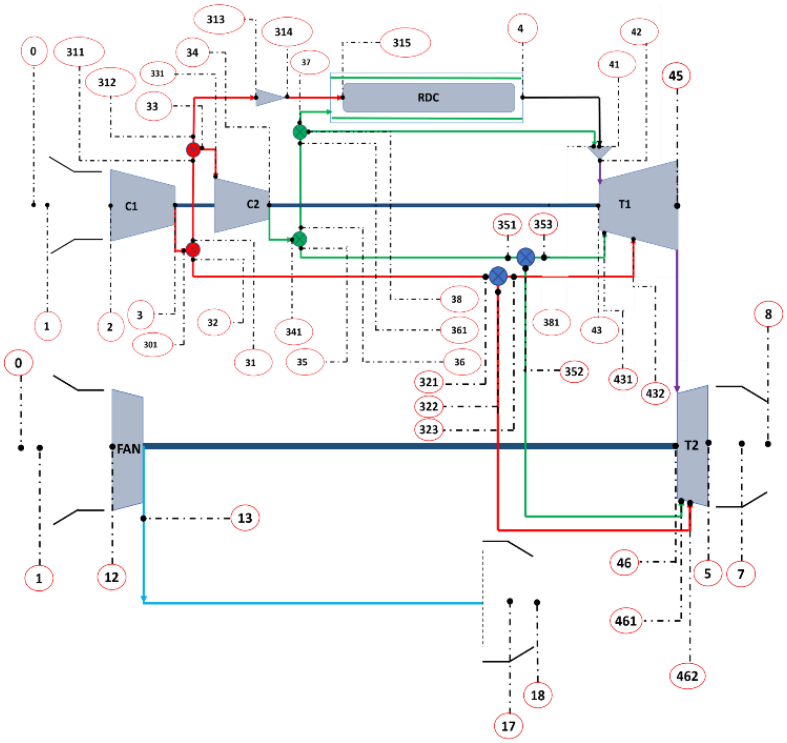

Fig. 7 Engine layout for a PGC engine for propulsion application

The operating map of the RDE combustor is generated using a modified version of Shock & Detonation toolbox [28]. For the present study, a mixture of hydrogen & air is considered with single wave operating mode of RDE combustor. The equilibrium chemical reaction calculation for hydrogen fuel with dry air is obtained using CANTERA [29] code, and the exit conditions of the RDE combustor are calculated under the assumption that the gases expand to a Mach number of 0.8 at the combustor exit at the selected design point, through gas dynamic phenomena typical to that seen in RDE combustor. This ensures that the flow is subsonic at the T1 inlet, with additional Mach number reduction to 0.5 using a subsonic diffuser passage in the mixer.

The fuel-air mixture flow suffers a stagnation pressure loss during injection into the RDE combustor, where the fresh charge layer encounters the detonation wave. Studies [30,31] have shown that this loss could be up to 50% for a good mixing efficiency. For the current study, this value is taken as 40%. The maps for compressor C1, fan and turbines T1 and T2 are those of the HPC, fan, HPT and LPT respectively, that are used in the CFM56-3 engine modelling with suitable scaling for the on-design condition of PGC engine. The booster compressor C2 has a pressure ratio of 2 and isentropic efficiency of 87% at on-design condition. The exhaust nozzles are the same for both engines as well.

The PGC engine is simulated at an on-design point to validate the capability of TRANSEO simulation tool to model such a complicated system. The results of both the conventional engine and PGC engine are discussed in the next section.

V. Results

A. Bleed & cooling layout selection for CFM56-3 engine modelling

In Type 1 bleed model, the HPT NGV and HPT rotor blade cooling air is provided upstream of HPT component while LPT NGV cooling air is provided upstream of LPT component (Fig.). Both the mass flow and enthalpies are balanced inside the bleed delivery control. The difference in the thermodynamic properties along the gas path are shown in Fig. for Type 1 (a) and Type 2 (b). In Type 2, the HPT NGV cooling air is provided upstream of HPT component, while the HPT rotor cooling air and LPT NGV cooling air supplies are provided between the HPT and LPT components, as shown in Fig. .

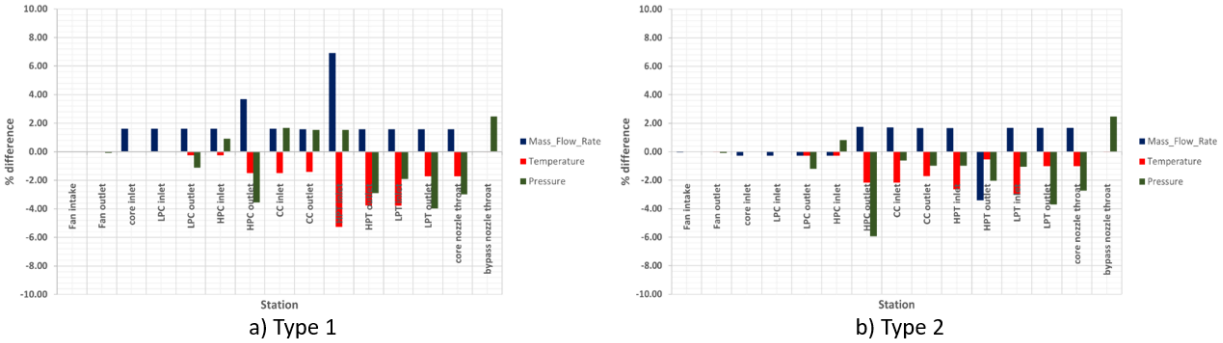

Fig. 8 Thermodynamic properties at engine stations for a) Type 1 and b) Type 2 models

Type 1 model produced an error of 1.033 % in net thrust and -1.018 % in thrust specific fuel consumption (TSFC) while Type 2 model produced an error of 1.205 % and -1.186 % for the same quantities. Therefore, the difference in the models is mainly on the differences in properties at the engine stations. From the figures, it is evident that Type 2 model is better suited for this type of engine, and hence it is selected for further studies.

B. On-design & off-design simulation of CFM56-3 engine

The TRANSEO engine model as shown in Fig. with Type 2 bleed model is simulated for a number of operating conditions and validated against the experimental results mentioned in [22].

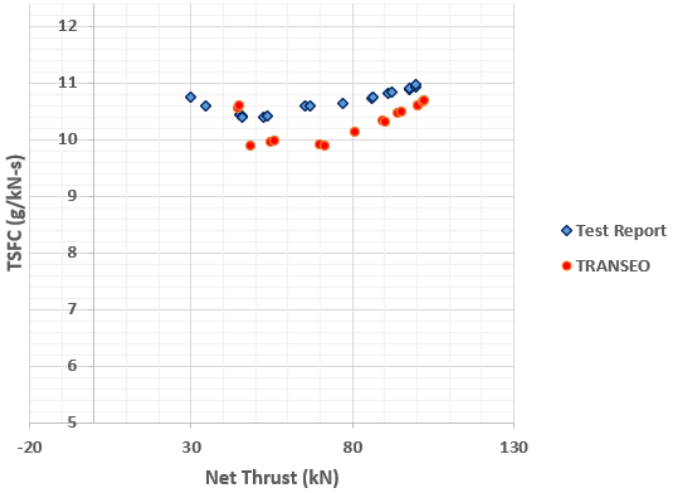

Fig. 9 Comparison of Net Thrust v/s TSFC

The results of the simulation are compared against the experimental values, and are shown in Fig. to Fig. 11. The net thrust and TSFC values are within 5% except at low mass flow rates. The same trend can be seen in temperatures as in Fig. a) – 8 d) and in pressures, as shown in Fig. 11 a) – 9 d). These variations can be attributed to the difference in bleed schedule at low engine speeds as compared to the data available at high engine speeds, the lack of interstage bleed and cooling facility in the TRANSEO turbomachinery components, and the compressor surge mitigation techniques that are not modelled in the TRANSEO simulation.

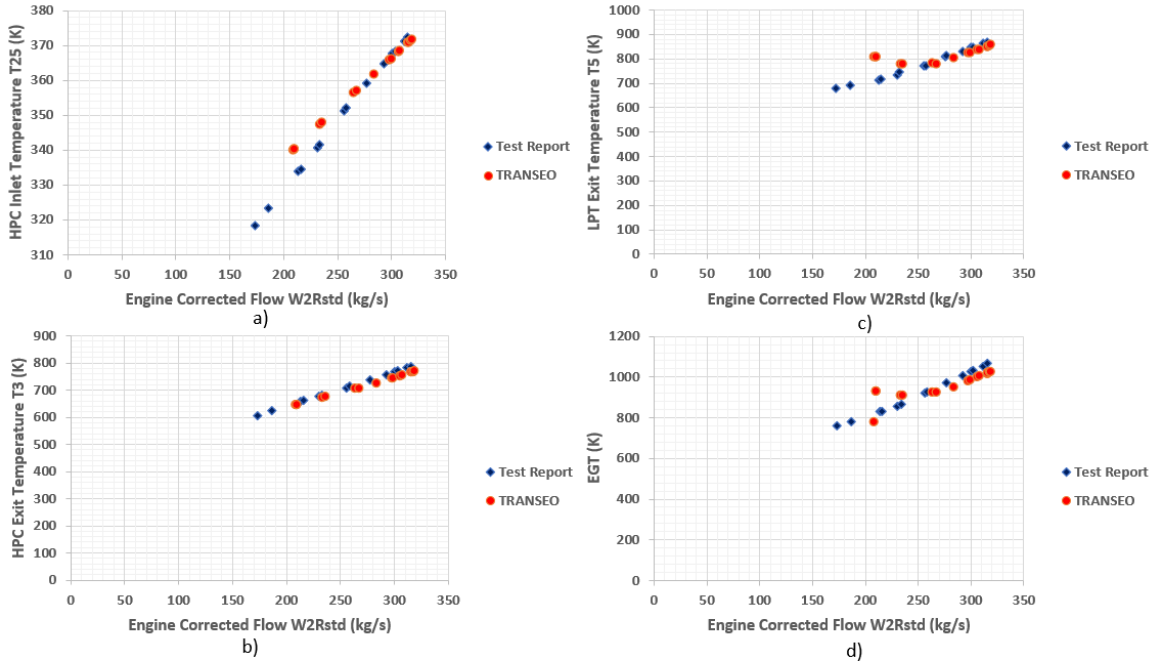

Fig. 10 Comparison of temperatures at different stations

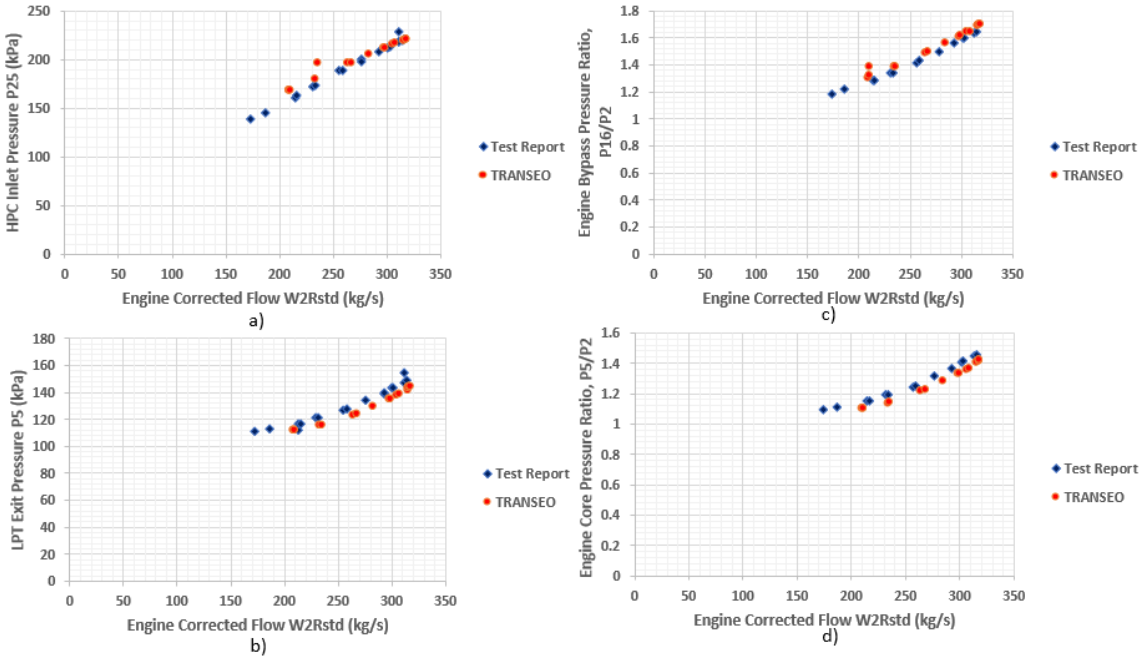

Fig. 11 Comparison of pressures at different stations

But from the perspective of an overall comparison, it can be concluded that the modelling technique employed using TRANSEO simulation tool is adequate enough to simulate a conventional aircraft engine [32].

C. RDE combustor modelling

Since TRANSEO simulation tool is developed to simulate the system level performance, the detailed fluid dynamic phenomenon and chemical reaction mechanisms are not required for the modelling of the RDE combustor. Instead, at this stage in the development of the engine model, a combustor map is generated (examples in Fig. and Fig.). The map uses static pressure and static temperature in the fresh mixture layer of the RDE combustor, the fuel-air equivalence ratio, and the exit Mach number of the combustor to obtain the exit stagnation pressure and stagnation temperature. The Mach number at the fresh mixture layer is assumed to be 1.0-1.1 (see [33] for an example of CFD results of rotating detonation wave propagation in a hydrogen - oxygen mixture). A supersonic injection regime may occur when pressure in the combustor is rather low, due to no restriction at the combustor exit. If a restriction is assumed, a subsonic injection regime could be obtained, with a Mach number of 0.5-0.8. The data for the map is validated using the method described in [34,35].

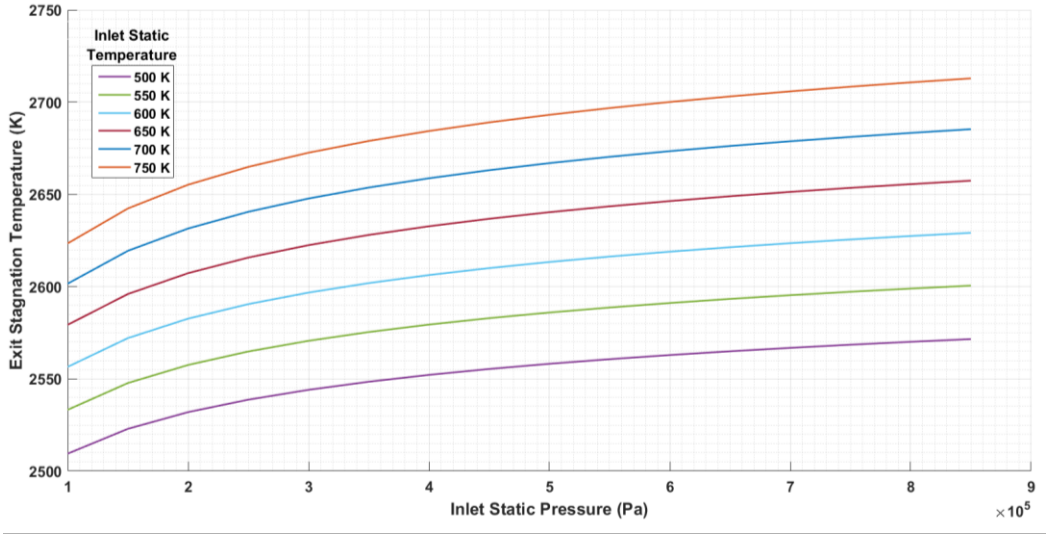

Fig. 12 RDE combustor temperature map for equivalence ratio 1 and exit Mach number 0.8.

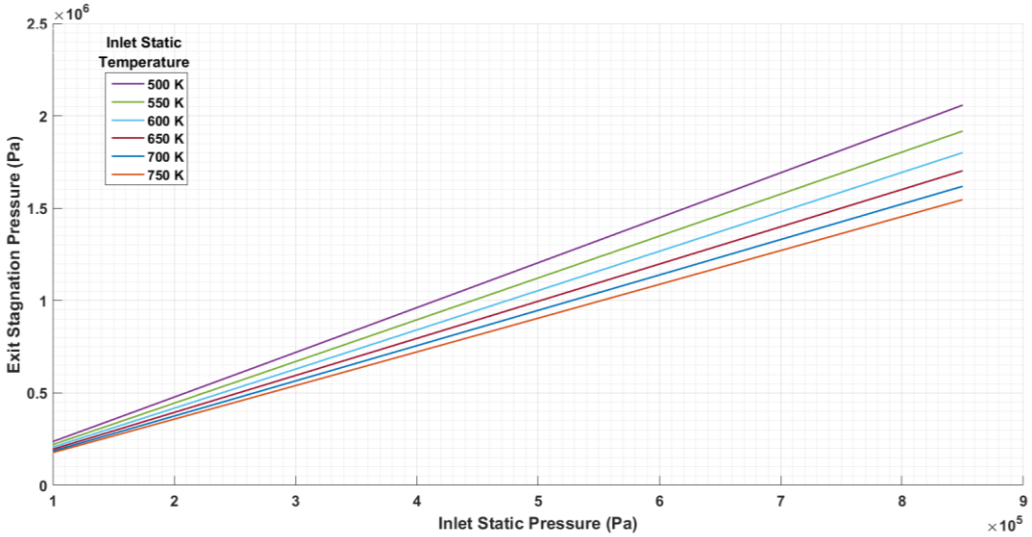

Fig. 13 RDE combustor pressure map for equivalence ratio 1 and exit Mach number 0.8.

D. On-design simulation of PGC engine

The layout shown in Fig. is modelled using TRANSEO as shown in Fig. . The fuel flow rate and splitter flow rates are set to obtain the same net thrust as the CFM56-3 engine model at the chosen design point.

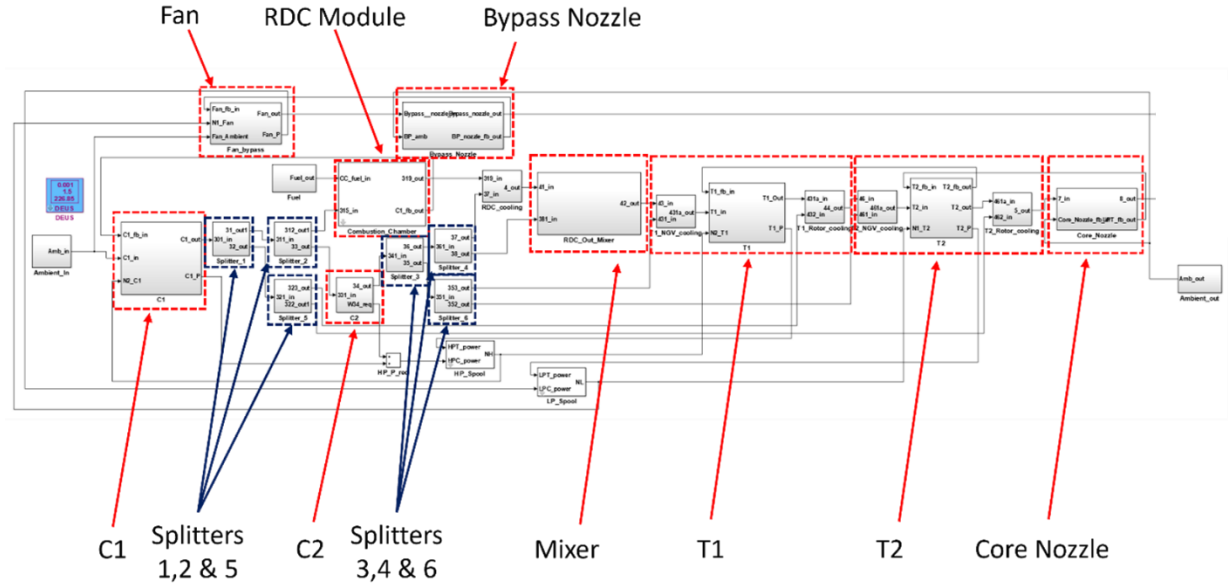

Fig. 14 PGC aircraft engine model in TRANSEO

The time - history evolution of mass flow rate and stagnation temperature at the throat of core nozzle and bypass nozzle are shown in Fig. . The results of the simulation are given in Table 1 and Table 2.

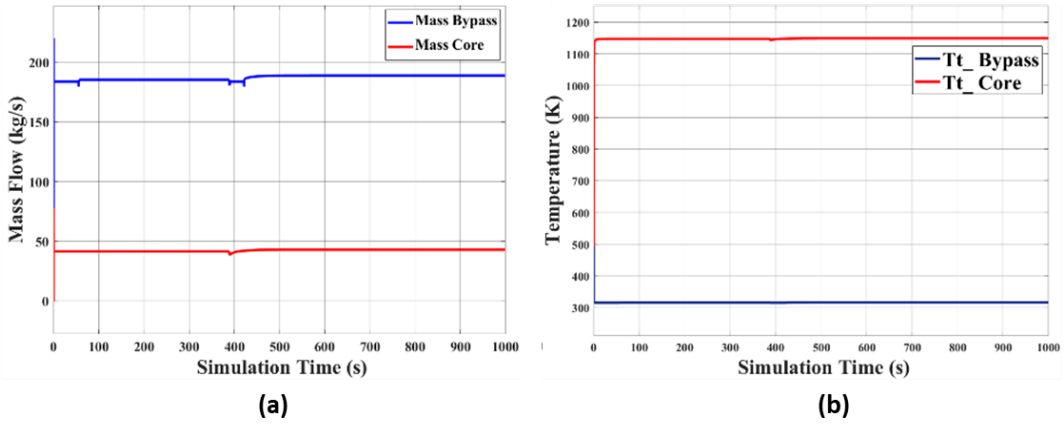

Fig. 15 Evolution of thermodynamic properties at core and bypass nozzles

Table 1 Comparison of performance of the PGC engine model with CFM56-3

	PGC	CFM56-3	% improvement with PGC
Net Thrust (kN)	94.215	94.215	NA
TSFC (g/kN)	4.2456	10.853	60.9%

Table 2 On-design simulation results for PGC engine model

Station No:	Station Details	Mass Flow Rate	Stagnation Pressure	Stagnation Temperature
		kg/s	bar	K
0	Ambient	0.00	1.01	288.15
12	Fan_in	182.92	1.01	288.15
13	Fan_out	182.92	1.35	316.62
2	C1_in	41.26	1.01	288.15
3	C1_out	41.26	10.13	607.76
31	Splitter 1_Primary	40.44	10.13	607.76
32	Splitter 1_Secondary	0.83	10.13	607.76
312	Splitter 2_Primary	18.20	10.13	607.76
33	Splitter 2_Secondary	22.24	10.13	607.76
331	C2_in	22.24	10.13	607.76
34	C2_out	22.24	20.27	752.63
35	Splitter 3_Secondary	0.67	20.27	752.63
36	Splitter 3_Primary	21.57	20.27	752.63
322	Splitter 5 to T2	0.33	10.13	607.76
323	Splitter 5 to T1	0.50	10.13	607.76
352	Splitter 6 to T2	0.20	20.27	752.63
353	Splitter 6 to T1	0.47	20.27	752.63
315	RDC_in	18.20	10.13	607.76
	Fuel flow_in	0.40	30.00	600.00
319	RDC_out	18.60	11.46	2308.81
37	RDC_cooling_in	6.47	20.27	752.63
4	CC_Post cooling	25.07	11.46	1986.06
41	Mixer_in	25.07	11.46	1986.06
38	Mixer_cooling_in	15.10	20.27	752.63
42	Mixer_out	40.17	11.46	1585.42
43	T1_in	40.17	11.46	1585.42
431	T1_NGV_cooling_in	0.47	20.27	752.63
432	T1_Rotor_cooling_in	0.50	10.13	607.76
45	T1_out	41.13	3.78	1257.22
46	T2_in	41.13	3.78	1257.22
461	T2_NGV_cooling_in	0.20	20.27	752.63
462	T2_Rotor_cooling_in	0.33	10.13	607.76
5	T2_out	41.66	2.55	1152.86
8	Hot Nozzle	41.66	2.55	1152.86
18	Cold Nozzle	182.92	1.35	316.62

The maps used for the CFM56-3 engine were scaled to handle the mass flow rate and pressure ratios required by the PGC engine. The scaling of the maps was done in the method described by Kurzke [36]. The geometries of the components were kept the same as in the case of CFM56-3 engine simulation. The splitting of mass flow at 6 different locations (referred to as 'splitter' in Fig. and Table 2) was done in such a way that the inlet stagnation temperatures of the turbines T1 & T2 are less than 1600 K and 1300 K respectively in adherence to the possible limitations on the turbine blade & guide vane materials. The turbine NGVs and rotor blade cooling are done similar to CFM56-3 engine model, with the addition of rotor cooling for T2 turbine.

The low-speed and high-speed spool shaft components are used to obtain turbine – compressor matching. The shaft component uses an approximate spool speed at the start of the simulation for numerical stability (provided by the user), and once the calculated speed satisfies a threshold value, the component delivers the calculated speed to the turbomachinery in the spool. This change in the user defined value to the calculated speed is visible in the time – history evolution of the mass flow rate and temperature at the core and bypass nozzle throats as a sudden jump (Fig.). The simulation is terminated when the change in the shaft speed is negligible [27]. The mechanical efficiencies of the shafts are maintained the same as in the CFM56-3 engine model.

It is to be noted that the pressure losses due to the mixing of hot and cold air are assumed to be negligible to simplify the model. In addition, the frictional loss and heat transfer for each component are also assumed similar to the CFM56-3 engine model. Also, the mixer component is defined as consisting of a diffuser passage which reduces the flow Mach number from 0.8 at the RDC exit to 0.5 at the turbine (T1) inlet and allows the mixing of fluids to reduce the turbine inlet temperature for T1.

In order to make a comparison between the conventional engine using constant pressure combustion and the new engine using PGC, the TSFC of the CFM56-3 engine is taken from Fig. for the same net thrust. Since the two engine models use different fuels, it is difficult to directly compare their performance. The widely used metrics such as net thrust and TSFC for the two engines are given in Table 1. From these figures, it can be seen that PGC has better TSFC than conventional engines. Further studies are warranted on this issue with better pressure loss models.

Table 2 shows the thermodynamic properties for the PGC engine at different stations in the cycle, as shown in Fig. . The engine, ideally designed for a bypass ratio of 5, is operating at a bypass ratio of 4.43. The inclusion of the booster compressor C2 in the layout to provide the high-pressure secondary air streams for cooling purpose seems to have an adverse effect on the performance, as the large pressure difference between station 38 & 42 (Mixer) indicate an inefficient use of fluid enthalpy. Similarly, the benefits of using the detonation combustor for pressure gain is overshadowed by the fuel-air injection pressure loss, as shown between stations 315 and 319. This along with the performance values indicates the need for components specifically tailored for PGC engines, rather than using the same turbomachinery components as in conventional engines, and a better optimized engine layout.

VI. Conclusion

This paper presents the overall system performance analysis of an aircraft engine, which utilizes pressure gain combustion instead of the conventional constant pressure combustion, focusing on the whole cycle behavior. The simulation performed using simplified component models demonstrates the capability of TRANSEO simulation tool to investigate both existing and novel propulsion cycles. The drawbacks of the existing component modules, such as interstage bleed, are identified and will be improved in further studies. This study also facilitates the improvement of the TRANSEO library for future studies involving full dynamic analysis of aircraft engines with pressure gain combustion. In addition, the results of the study demonstrate the necessity to improve the current PGC engine layout to obtain better performance.

Acknowledgments

This project has received funding from the European Union's Horizon 2020 research and innovation programme under the Marie Skłodowska-Curie grant agreement No: INSPIRE-956803.

References

[1] Heiser, W. H., and Pratt, D. T. "Thermodynamic Cycle Analysis of Pulse Detonation Engines." *Journal of Propulsion and Power*, Vol. 18, No. 1, 2002, pp. 68–76. https://doi.org/10.2514/2.5899.

[2] Stathopoulos, P. "Comprehensive Thermodynamic Analysis of the Humphrey Cycle for Gas Turbines with Pressure Gain Combustion." *Energies*, Vol. 11, No. 12, 2018. https://doi.org/10.3390/en11123521.

[3] Purushothaman, S., Renuke, A., Sorce, A., and Traverso, A. "A Review of Pressure Gain Combustion Solutions for Aerospace Propulsion." *Turbo Expo: Power for Land, Sea, and Air*, Vol. 86014, 2022, p. V004T06A035.

[4] Stathopoulos, P. “An Alternative Architecture of the Humphrey Cycle and the Effect of Fuel Type on Its Efficiency.” *Energy Science and Engineering*, Vol. 8, No. 10, 2020. https://doi.org/10.1002/ese3.776.

[5] Stathopoulos, P., Rähse, T., Vinkeloe, J., and Djordjevic, N. “First Law Thermodynamic Analysis of the Recuperated Humphrey Cycle for Gas Turbines with Pressure Gain Combustion.” *Energy*, Vol. 200, 2020, p. 117492. https://doi.org/10.1016/J.ENERGY.2020.117492.

[6] Stechmann, D. P., Heister, S. D., and Harroun, A. J. Rotating Detonation Engine Performance Model for Rocket Applications. No. 56, 2019.

[7] Okninski, A., Kindracki, J., and Wolanski, P. “Rocket Rotating Detonation Engine Flight Demonstrator.” *Aircraft Engineering and Aerospace Technology*, Vol. 88, No. 4, 2016, pp. 480–491. https://doi.org/10.1108/AEAT-07-2014-0106.

[8] Nishimura, J., Ishihara, K., Goto, K., Nakagami, S., Matsuoka, K., Kasahara, J., Matsuo, A., Funaki, I., Mukae, H., and Yasuda, K. Performance Evaluation of a Rotating Detonation Engine for Space Use. 2017.

[9] Goto, K., Matsuoka, K., Matsuyama, K., Kawasaki, A., Watanabe, H., Itouyama, N., Ishihara, K., Buyakofu, V., Noda, T., Kasahara, J., Matsuo, A., Funaki, I., Nakata, D., Uchiumi, M., Habu, H., Takeuchi, S., Arakawa, S., Masuda, J., Maehara, K., Nakao, T., and Yamada, K. Flight Demonstration of Detonation Engine System Using Sounding Rocket S-520-31: Performance of Rotating Detonation Engine. In *AIAA SCITECH 2022 Forum*, American Institute of Aeronautics and Astronautics, 2021.

[10] Naples, A., Hoke, J., Battelle, R. T., Wagner, M., and Schauer, F. R. RDE Implementation into an Open-Loop T63 Gas Turbine Engine. 2017.

[11] Naples, A., Hoke, J., Battelle, R., and Schauer, F. “T63 Turbine Response to Rotating Detonation Combustor Exhaust Flow.” *Journal of Engineering for Gas Turbines and Power*, Vol. 141, No. 2, 2019. https://doi.org/10.1115/1.4041135.

[12] Paxson, D. E., and Naples, A. Numerical and Analytical Assessment of a Coupled Rotating Detonation Engine and Turbine Experiment. 2017.

[13] Borys, Ł., Czyż, S., Irzycki, A., and Rowiński, A. “The Study of the Continuously Rotating Detonation Combustion Chamber Supplied with Different Types of Fuel.” *Journal of KONES Powertrain and Transport*, 2013.

[14] Kindracki, J. “Experimental Research on Rotating Detonation in Liquid Fuel-Gaseous Air Mixtures.” *Aerospace Science and Technology*, Vol. 43, 2015, pp. 445–453. https://doi.org/10.1016/j.ast.2015.04.006.

[15] Dubey, A., Purushothaman, S., Sorce, A., and Traverso, A. A Review of Recent Advances in the Combustor and Blade Cooling Methods for Pressure Gain Applications. *Joint Meeting of International Workshop on Detonation for Propulsion (IWDP) and International Constant Volume and Detonation Combustion Workshop (ICVDCW)*.

[16] Alexiou, A., and Mathioudakis, K. Gas Turbine Engine Performance Model Applications Using an Object-Oriented Simulation Tool. No. 42371, 2006, pp. 109–116.

[17] Khalil, E. E., El-Sayed, A. F., and Abdelghany, E. S. Effect of Bleed Air on Performance of Turbofan Engines. 2013.

[18] Sankar, B., Subramanian, T., Shah, B., Vanam, V., Jana, S., Ramamurthy, S., Satpathy, R., Sahoo, B., and Yadav, S. Aero-Thermodynamic Modelling and Gas Path Simulation for a Twin Spool Turbo Jet Engine. 2013.

[19] Carcasci, C., Piola, S., Canepa, R., and Silingardi, A. Gas Turbine Integrated Conceptual Design Approach. No. 3, 2015.

[20] Carcasci, C., Facchini, B., Gori, S., Bozzi, L., and Traverso, S. “Heavy Duty Gas Turbine Simulation: Global Performances Estimation and Secondary Air System Modifications.” *Turbo Expo: Power for Land, Sea, and Air*, Vol. 42398, 2006, pp. 527–536.

[21] Martins, D. A. R. “Off-Design Performance Prediction of the Cfm56-3 Aircraft Engine.” *Tecnico Lisboa MSc Thesis*, 2015.

[22] Ridaura, J. A. R. “Correlation Analysis between HPC Blade Chord and Compressor Efficiency for the CFM56-3.” *Portugal: sn*, 2014.

[23] Traverso, A. TRANSEO Code for the Dynamic Performance Simulation of Micro Gas Turbine Cycles. No. 5, 2005.

[24] Traverso, A., Massardo, A. F., and Scarpellini, R. “Externally Fired Micro-Gas Turbine: Modelling and Experimental Performance.” *Applied Thermal Engineering*, Vol. 26, No. 16, 2006. https://doi.org/10.1016/j.applthermaleng.2006.01.013.

[25] Ferrari, M. L., Liese, E., Tucker, D., Lawson, L., Traverso, A., and Massardo, A. F. “Transient Modeling of the NETL Hybrid Fuel Cell/Gas Turbine Facility and Experimental Validation.” *Journal of Engineering for Gas Turbines and Power*, Vol. 129, No. 4, 2007. https://doi.org/10.1115/1.2747265.

[26] Lambruschini, F., Liese, E., Zitney, S. E., and Traverso, A. Dynamic Model of a 10 Mw Supercritical CO2 Recompression Brayton Cycle. No. 9, 2016.

[27] Traverso, A. *TRANSEO: A New Simulation Tool for Transient Analysis of Innovative Energy Systems: PhD Thesis*. University of Genova, Genova, Italy, 2004.

[28] Browne, S., Ziegler, J., and Shepherd, J. E. *Numerical Solution Methods for Shock and Detonation Jump Conditions*. 2008.

[29] Goodwin, D. G. CANTERA: An Open-Source, Object-Oriented Software Suite for Combustion. *NSF Workshop on Cyber-based Combustion Science*.

[30] Suzuki, T., Matsuo, A., Daimon, Y., Kawashima, H., Kawasaki, A., Matsuoka, K., and Kasahara, J. Prediction of Pressure Loss in Injector for Rotating Detonation Engines Using Single-Element Simulations. 2020.

[31] Gaillard, T., Davidenko, D., and Dupoirieux, F. “Numerical Optimisation in Non Reacting Conditions of the Injector Geometry for a Continuous Detonation Wave Rocket Engine.” *Acta Astronautica*, Vol. 111, 2015. https://doi.org/10.1016/j.actaastro.2015.02.006.

[32] Purushothaman, S., Sorce, A., and Traverso, A. *Test of TRANSEO Code, Equipped with Literature Performance Maps*. 2022.

[33] Gaillard, T., Davidenko, D., and Dupoirieux, F. “Numerical Simulation of a Rotating Detonation with a Realistic Injector Designed for Separate Supply of Gaseous Hydrogen and Oxygen.” *Acta Astronautica*, Vol. 141, 2017. https://doi.org/10.1016/j.actaastro.2017.09.011.

[34] Davidenko D., Gökalp I., F. F. “Theoretical Performance of Rocket and Turbojet Engines Operating in the Continuous Detonation Mode.” *4th European Conference for Aerospace Sciences (EUCASS)*, 2011.

[35] Davidenko, D. M., Eude, Y., Gökalp, I., and Falempin, F. Theoretical and Numerical Studies on Continuous Detonation Wave Engines. 2011.

[36] Kurzke, J. How to Create a Performance Model of a Gas Turbine from a Limited Amount of Information. No. 1, 2005.